PNAS RESEARCH ARTICLE | NEUROSCIENCE OPEN ACCESS

# Modified climbing fiber/Purkinje cell synaptic connectivity in the cerebellum of the neonatal phencyclidine model of schizophrenia

Maxime Veleanu[a,1], Beetsi Urrieta-Chávez[a,1], Séverine M. Sigoillot[a,1], Maëla A. Paul[a], Alessia Usardi[a], Keerthana Iyer[a], Marine Delagrange[b], Joseph P. Doyle[c,d], Nathaniel Heintz[c,d,2], Carine Bécamel[e], and Fekrije Selimi[a,2]

Contributed by Nathaniel Heintz; received December 16, 2021; accepted March 23, 2022; reviewed by Harry Orr and Roy Sillitoe

**Environmental perturbations during the first years of life are a major factor in psychiatric diseases. Phencyclidine (PCP), a drug of abuse, has psychomimetic effects, and neonatal subchronic administration of PCP in rodents leads to long-term behavioral changes relevant for schizophrenia. The cerebellum is increasingly recognized for its role in diverse cognitive functions. However, little is known about potential cerebellar changes in models of schizophrenia. Here, we analyzed the characteristics of the cerebellum in the neonatal subchronic PCP model. We found that, while the global cerebellar cytoarchitecture and Purkinje cell spontaneous spiking properties are unchanged, climbing fiber/Purkinje cell synaptic connectivity is increased in juvenile mice. Neonatal subchronic administration of PCP is accompanied by increased cFos expression, a marker of neuronal activity, and transient modification of the neuronal surfaceome in the cerebellum. The largest change observed is the overexpression of *Ctgf*, a gene previously suggested as a biomarker for schizophrenia. This neonatal increase in *Ctgf* can be reproduced by increasing neuronal activity in the cerebellum during the second postnatal week using chemogenetics. However, it does not lead to increased climbing fiber/Purkinje cell connectivity in juvenile mice, showing the complexity of PCP action. Overall, our study shows that administration of the drug of abuse PCP during the developmental period of intense cerebellar synaptogenesis and circuit remodeling has long-term and specific effects on Purkinje cell connectivity and warrants the search for this type of synaptic changes in psychiatric diseases.**

synapse | cerebellum | development | schizophrenia | phencyclidine

## Significance

Synaptogenesis and neural network remodeling are at their maximum during the perinatal period of human brain development. Perturbations of this highly sensitive stage might underlie the etiology of neurodevelopmental disorders. Subchronic neonatal administration of phencyclidine, a drug of abuse, has been used to model schizophrenia in rodents. In this model, we found specific long-term synaptic changes in Purkinje cells and transient gene expression changes in the cerebellum. While transient increased neuronal activity in the cerebellum, induced using chemogenetics, reproduces some phencyclidine-induced molecular changes, it is insufficient to reproduce the long-term synaptic effects. Our results show the complex mechanism of action of phencyclidine on the development of neuronal connectivity and further highlight the potential contribution of cerebellar defects in psychiatric diseases.

Phencyclidine (PCP), a noncompetitive *N*-methyl-D-aspartate (NMDA) receptor antagonist initially developed for its properties as an anesthetic, became a popular drug of abuse in the 1960s (1, 2). Nowadays, PCP is often mixed with other drugs, in particular marijuana, and a US 2013 report estimated that PCP-related emergency department visits increased more than 400% between 2005 and 2011 (https://www.samhsa.gov/data/sites/default/files/DAWN143/DAWN143/sr143-emergency-phencyclidine-2013.htm). PCP has important psychotomimetic effects, such as alterations of body image, feelings of estrangement and loneliness, and disorganization of thought. Repeated use of PCP induces persistent symptoms found in schizophrenia, including both positive (hallucinations, psychosis …), cognitive and negative (social withdrawal) effects. PCP also produces regressive symptoms in schizophrenic patients. These observations led to the NMDA hypothesis of schizophrenia and the development of animal models using both acute and chronic PCP administration to study the pathophysiology of this disease (3). Because schizophrenia is now considered a developmental disorder, neonatal administration of PCP in rodents has been tested and shown to produce a wide range of behavioral alterations in the adult, including spatial memory deficits (4, 5) and a deficit in social novelty discrimination (6–8). Some studies found defects in prepulse inhibition (PPI) of the startle response, a sensorimotor gating task used both in animal models and in humans as a behavioral marker of psychiatric disorders (4, 9, 10). Interestingly, these PPI deficits last even after withdrawal, which is not the case when PCP is administered in adulthood, suggesting that this aspect of the disease is better modeled by neonatal administration of PCP. Finally, PCP abuse during pregnancy has been associated with neurobehavioral defects (11) and with long-term consequences on social behavior and motor control in children (12), further highlighting the need to understand the consequences of PCP exposure on the development of neuronal networks.

In the subchronic neonatal PCP model, the drug is administered three times during the second postnatal week in rodents (Fig. 1*A*), a period of intense neuronal growth and synaptogenesis. This developmental stage is particularly sensitive to early

Reviewers: H.O., University of Minnesota Medical School; and R.S., Baylor College of Medicine.

The authors declare no competing interest.



[1]M.V., B.U.-C., and S.M.S. contributed equally to this work.

[2]To whom correspondence may be addressed. Email: heintz@rockefeller.edu or fekrije.selimi@college-de-france.fr.

This article contains supporting information online at http://www.pnas.org/lookup/suppl/doi:10.1073/pnas.2122544119/-/DCSupplemental.

Published May 19, 2022.

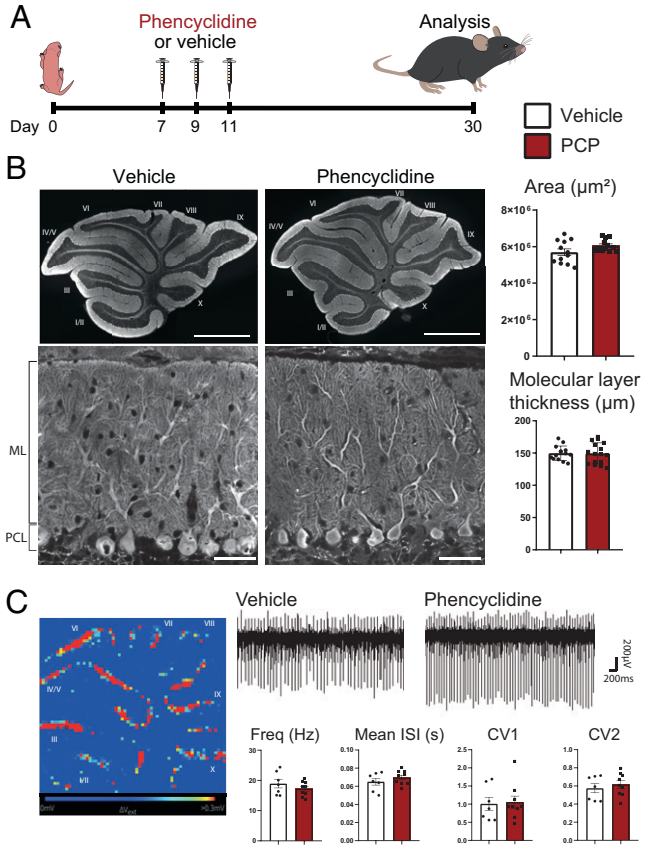


**Fig. 1.** Neonatal PCP administration does not modify the cytoarchitecture of the cerebellum and the spontaneous activity of PCs. (*A*) Experimental design. PCP (10 mg/kg) or vehicle is injected subcutaneously in mouse pups at P7, P9, and P11. Morphological and electrophysiological analyses are performed at P30. (*B*) Parasagittal cerebellar sections from the vermis of P30 mice were immunolabeled with an anti-calbindin antibody to stain PCs in their entirety and reveal cerebellar cytoarchitecture. Quantification of the mean area of cerebellar slices showed no significant differences between the two conditions (mean ± SEM; vehicle: $n = 12$ animals; PCP: $n = 12$; $P = 0.0962$, Student's $t$ test). Representative images from PCs and their dendritic tree in lobule VI reveal similar morphology in sections from P30 vehicle- and PCP-treated animals. Quantification of the thickness of the molecular layer (ML) in the lobule VI, measured as the length from the beginning of the primary dendrite of PCs in the Purkinje cell layer (PCL) to the upper extremity of the ML, reveals no significant difference between vehicle- and PCP-treated animals (lobule VI is shown here; mean ± SEM; vehicle: $n = 14$ animals; PCP: $n = 16$ animals; $P = 0.964$, unpaired Student's $t$ test). (Scale bars: *Upper*, 1,000 µm; *Lower*, 50 µm.) (*C*) High-density MEAs were used to record PC spontaneous spiking in acute cerebellar slices from P30 mice. An example of the recorded electrical activity in a cerebellar slice from a vehicle-treated mouse is shown with each pixel representing one channel and units showing high activity in red and low activity in blue. A representative trace of recordings from one channel is shown for each condition. Spike sorting using the SpyKING CIRCUS software allowed for estimation of the mean firing rate and mean interspike interval (ISI) CV and CV2. No significant difference was detected in any of these parameters (mean ± SEM; vehicle: $n = 7$ animals; PCP, $n = 9$ animals; unpaired Student's $t$ test).

environmental stressors associated with increased risk of developing schizophrenia in humans (13). Histopathological and genetic studies have revealed that schizophrenia is a synaptopathy. Mutations and expression changes have been found in genes coding for synaptic proteins (14–19) (a meta-analysis is in ref. 20). Postmortem studies of the cortex of patients with schizophrenia have revealed deficits in dendritic arborization, spine densities, and the number of parvalbumin interneurons (21–25). Similar spine and cellular deficits have been reported in the PCP neonatal model (5, 26, 27), as well as impaired function of both excitatory and inhibitory synapses (28–30). It is, however, still unclear whether these common alterations in schizophrenia and the neonatal PCP model are due to the direct inhibition of NMDA function or a complex interaction between perturbations of neuronal activity and genetic factors.

While initially thought to be a motor-related structure, it is now well established that the cerebellum also plays a role in cognitive processes (31, 32), such as spatial navigation (33), language (34), reward (35), and social cognition (36). In addition, while schizophrenia has been primarily thought of as a disease of the prefrontal cortex or hippocampus, the cerebellum has emerged as a potential actor in this pathology. Schizophrenic patients often present a decreased cerebellar volume (37–39) as well as neurological soft signs, a type of sensorimotor impairment that implicates the cerebellum (40). Interestingly, neurological soft signs have been correlated with a poor outcome and greater negative and cognitive symptoms (41–43). A significant correlation between negative symptoms in schizophrenia and diminished connectivity between the dorsolateral prefrontal cortex and vermal posterior cerebellum was found in a study of whole-brain connectivity using resting-state functional magnetic resonance imaging in schizophrenic patients (44). It is, however, still unknown whether synaptic deficits are present in the cerebellum of schizophrenic patients.

NMDA receptors are present in many neurons of the olivocerebellar circuit, such as molecular layer interneurons (45), granule cells (GCs) (46, 47), inferior olivary neurons (IONs) (48), and Purkinje cells (PCs) themselves (49). In the cerebellum, NMDA receptors participate in the control of neuronal survival (50), circuit maturation, and function (51–53), suggesting that neonatal administration of PCP, an NMDA antagonist, could directly impact the development of the olivocerebellar circuit. In this study, we combined morphological, electrophysiological, and molecular approaches to study the olivocerebellar network in the PCP neonatal model. Lasting synaptic changes were detected in juvenile mice, in particular at the climbing fiber (CF)/PC excitatory synapses, which are key for cerebellar computation. PCP was also found to induce a transient misregulation of the expression pattern of genes coding for membrane and secreted proteins in the cerebellum. The largest misregulation was found for *connective tissue growth factor* (*Ctgf*), a gene previously documented as a biomarker in schizophrenic patients. Reproducing the transient misregulation of *Ctgf* during the second postnatal week using chemogenetics was not sufficient to recapitulate the long-term synaptic changes induced by PCP in the olivocerebellar network. Altogether, neonatal subchronic administration of PCP leads to acute changes in gene expression and long-term synaptic connectivity modifications in the olivocerebellar circuit.

## Results

**Global Cerebellar Cytoarchitecture and Spontaneous Spiking Properties of PCs Are Normal in Juvenile Mice Treated Neonatally with PCP.** A decreased cerebellar volume is often found in schizophrenic patients (for review, see ref. 54). Morphological analysis of the global cytoarchitecture of the cerebellum in mice treated subchronically during the second postnatal week with PCP did not reveal any change compared with the one of vehicle-treated mice at a stage when the development of the cerebellum is completed (postnatal day 30 [P30]) (Fig. 1*B*). Calbindin immunostaining of cerebellar parasagittal sections, staining the whole dendritic arborization, soma, and axon of PCs, revealed the stereotypical organization of the cerebellar cortex in layers: the white matter, the internal granular layer, the monolayer of PC somata, and the molecular layer (Fig. 1*B*).

The molecular layer contains the dendritic tree of PCs, which receives all the excitatory inputs, from parallel fibers (PFs) and CFs, and the inhibitory inputs from stellate cells, also located in the molecular layer. Quantification showed no change in the surface of parasagittal vermal sections of the cerebellum or in the mean thickness of the molecular layer (Fig. 1*B*). While a previous study reported a deficit in parvalbumin cells in the brain of PCP-treated rodents (5), our quantification did not reveal any change in parvalbumin expression and density of inhibitory interneurons in the cerebellum of PCP-treated mice (*SI Appendix*, Fig. S1). Altogether, these quantifications support the absence of major deficits in interneurons, GC and PC genesis, and differentiation after neonatal subchronic PCP treatment. The firing pattern of PCs is characterized by simple spikes and complex spikes. GC inputs modulate the frequency of simple spikes and control the acquisition of a mature firing pattern during postnatal development (55). Spontaneous PC spiking activity was recorded in acute cerebellar slices from PCP mice and compared with controls using high-resolution microelectrode arrays (MEAs) (Fig. 1*C*). Spike sorting using SpyKING CIRCUS allowed for estimations of the mean firing rate (representing the mean activity of each recorded neuron), the coefficient of variation (CV; measuring the mean variance of interspike intervals during the whole recording), and CV2 (measuring the variability of spiking between two adjacent interspike intervals) (56). None of these parameters showed any statistically significant difference between PCP-treated and control mice (Fig. 1*C*). Altogether, these results show that neonatal PCP treatment does not affect the development of the cytoarchitecture of the cerebellar cortex and the differentiation of cerebellar PCs in a major and long-lasting manner.

**Neonatal PCP Treatment Induces Afferent-Specific Synaptic Deficits in Cerebellar PCs.** PCs receive two excitatory inputs, the CFs coming from IONs in the brainstem and the PFs coming from the GCs in the granular layer of the cerebellar cortex, and two inhibitory inputs coming from stellate and basket cells in the molecular layer. To analyze potential long-term synaptic deficits induced by neonatal PCP administration, we performed immunolabeling followed by high-resolution confocal microscopy and quantitative analysis for markers specific to the presynaptic terminal of each of these afferents on cerebellar sections from P30 animals. Because of the functional topography found in the cerebellum (57), we focused our quantitative morphological analysis on lobules engaged in various functions relevant for schizophrenia: lobule VI (language tasks, working memory paradigms, and spatial navigation) and lobule VIII (sensorimotor tasks) (32).

During the second postnatal week, the CF translocates along the dendritic tree of its target PC to form a few hundred synapses (presynaptic boutons labeled using the specific vesicular glutamate transporter 2 [VGLUT2] marker) (Fig. 2*A*) along the proximal dendrites. Its final territory extends up to ∼80% of the height of the molecular layer. In lobule VI, the extension of the CF synaptic territory was unchanged in PCP- vs. vehicle-treated mice, while in lobule VIII, a small (7%) but statistically significant increase in the extension of CF synaptic territory was detected (ratios relative to PC height are presented as mean ± SEM; lobule VIII: vehicle: mean ± SEM = 0.725 ± 0.012, $n = 14$; PCP: 0.781 ± 0.006, $n = 16$; $P = 0.0006$, Welch's $t$ test) (Fig. 2*A*). The density of the VGLUT2 puncta was significantly increased by 33% in lobule VI (mean number per cubic micrometer ± SEM; vehicle: 0.003 ± 0.0001, $n = 14$; PCP: 0.004 ± 0.0002, $n = 15$; $P = 0.0039$, Welch's $t$ test) (Fig. 2*A*), while it remained unchanged in lobule VIII. Our three-dimensional (3D) quantitative analysis of VGLUT2 puncta also revealed a general 20% decrease in the mean volume in PCP-treated mice compared with vehicle in both lobules (for lobule VI, vehicle: mean volume in micrometer cubed ± SEM = 1.796 ± 0.124, $n = 14$; PCP: 1.395 ± 0.078, $n = 14$; $P = 0.0114$, unpaired Student's $t$ test; for lobule VIII: vehicle: 1.429 ± 0.097, $n = 13$; PCP: 1.171 ± 0.059, $n = 15$; $P = 0.0283$, unpaired Student's $t$ test) (Fig. 2*A*). Altogether, these results demonstrate an overall decrease in the volume of VGLUT2-labeled presynaptic boutons and an increase in their total number. The magnitude of the increase in the number of VGLUT2 presynaptic boutons is higher in lobule VI, where it is the consequence of increased density, while the small increase in lobule VIII is due to increased synaptic territory. This shows a lobule-specific effect on CF/PC synaptic connectivity. The other excitatory afferent, the PFs, forms densely packed synapses with PC spines via small VGLUT1-positive presynaptic boutons (*SI Appendix*, Fig. S2*A*). As a proxy for synapse density, we measured the mean intensity of VGLUT1 labeling in the molecular layer (58) and found no difference between PCP- and vehicle-treated mice (*SI Appendix*, Fig. S2*A*). While alterations of glutamatergic synapses are one of the most widely highlighted physiopathological deficits in schizophrenia, there is also evidence for inhibitory deficits (59, 60). We also analyzed inhibitory synapses using GAD65 immunostaining of cerebellar sections. A similar pattern of inhibitory innervation was found in PCP-treated mice and in control animals; big boutons were observed around the soma and axon initial segment of PCs, corresponding to the basket cell innervation, and small GAD65-positive boutons were found in the molecular layer on the dendrite of PCs, corresponding to synapses from stellate cells. The 3D quantification did not show any change in the density or volume of inhibitory boutons in the molecular layer (*SI Appendix*, Fig. S2*B*). Altogether, these results point to a long-term effect of the PCP neonatal treatment on one particular synapse type made on cerebellar PCs, the CF/PC synapses, with an increased total number accompanied by a decrease in the volume of the CF presynaptic boutons.

To further analyze the long-term effect of PCP neonatal treatment on CF/PC connectivity, we performed patch-clamp recordings of PC responses to CF stimulation using acute cerebellar slices from P24 to P28 animals. We focused on lobule VI to determine whether the morphological changes identified at the CF/PC synapses were associated with changes in synaptic transmission. The responses to CF stimulation are characterized by a strong, all-or-none excitatory postsynaptic current (EPSC) that is depressed by paired-pulse stimulation (61). CF responses with the characteristic paired-pulse depression were detected in PCs of both PCP- and vehicle-treated animals. Paired-pulse depression was of similar magnitude across the interstimulus intervals tested (Fig. 2*B*), showing that short-term plasticity of the CF/PC synapse is not affected by PCP neonatal treatment. Interestingly, the mean values for the charge transfer, amplitude, and kinetics of the CF/PC EPSCs were not statistically different between PCP- and vehicle-treated animals (Fig. 2*B* and *SI Appendix*, Fig. S3), but a different distribution of the mean charge was evident. In the PCP-treated condition, the distribution spanned a larger range, with a subpopulation of PCs responding with a much higher charge transfer to CF stimulation. This result, together with our morphological analysis of CF synaptic boutons, indicates that PCP exposure during the second postnatal week increases CF connectivity and transmission in a subgroup of PCs, in particular in lobule VI, in juvenile animals. Thus, exposure to NMDA antagonists like

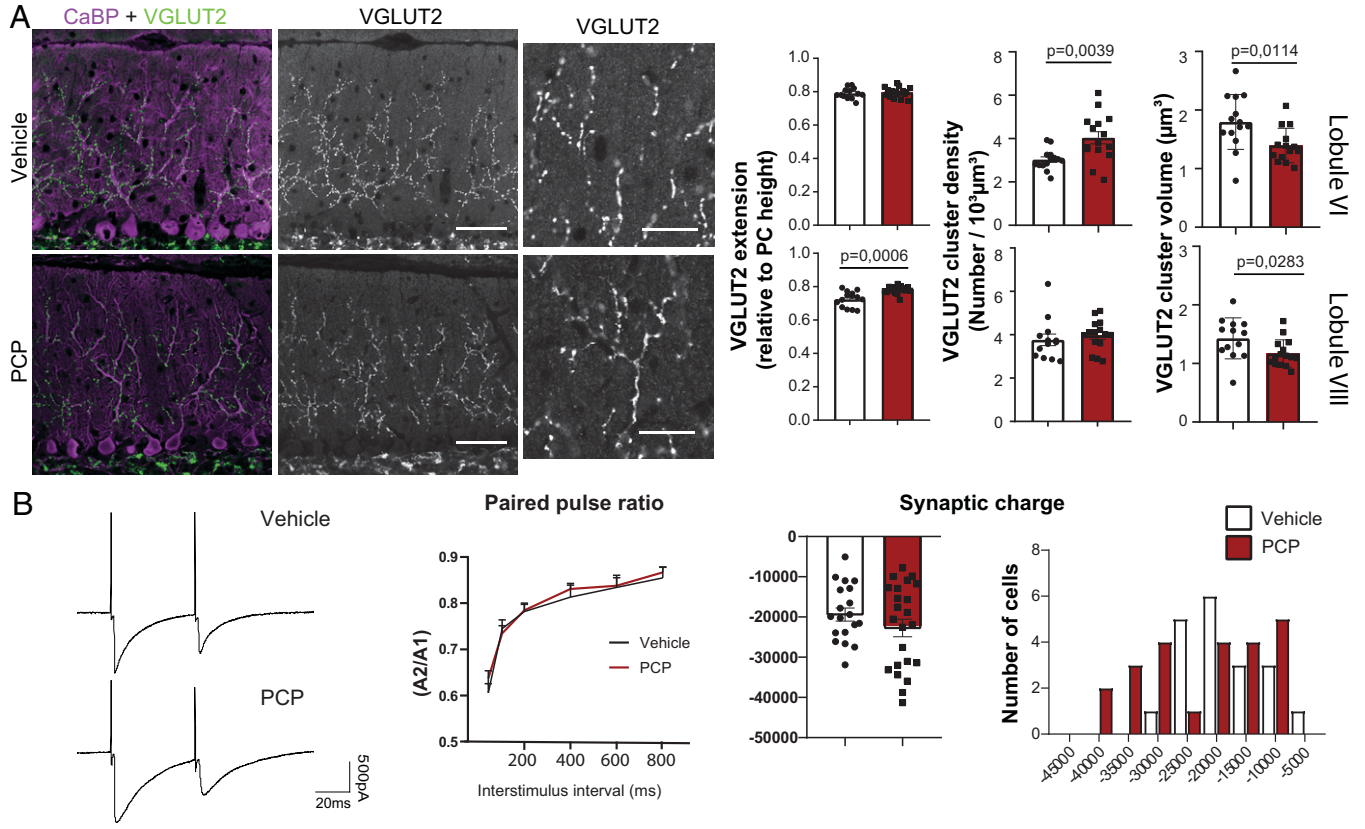


**Fig. 2.** Neonatal PCP administration leads to long-lasting changes in CF/PC connectivity. (*A*) CF presynaptic boutons were immunostained with an anti-VGLUT2 antibody (green) and PCs and their dendritic tree were stained with an anti-calbindin antibody (magenta) in parasagittal cerebellar sections from P30 vehicle- and PCP-treated mice. High-magnification images of VGLUT2 clusters are shown for both conditions. Quantifications of the extension of the CF synaptic territory, mean volume of the VGLUT2 puncta, and their mean density were performed in lobules VI and VIII (mean ± SEM is represented, with *P* values when they are significant; unpaired Student's *t* test for the volume, Welch's *t* test for the extension and density; vehicle: $n = 13$ to 14 animals; PCP: $n = 15$ to 16 animals). (Scale bars: 50 µm; high-magnification images, 20 $\mu$m.) (*B*) PC responses after CF stimulation were recorded using patch clamp. Representative traces of responses obtained in PCs from lobule VI after paired-pulse stimulation (50-ms interval) are shown for both conditions. No difference in the paired-pulse ratio (ratio between the amplitude of the second response and the first response A2/A1) was detected regardless of the stimuli interval between PCP mice and vehicle mice (Kolmogorov–Smirnov test). The mean synaptic charge after CF stimulation is not significantly different between the PCP and vehicle conditions (vehicle: $n = 19$ cells/9 mice and PCP: $n = 23$ cells/9 mice; unpaired Student's *t* test), but a change in the distribution is visible with a shift toward higher charges in the PCP condition.

PCP during the synaptogenic period of olivocerebellar network development could have a long-term effect on cerebellar computation in certain lobules that are relevant for psychiatric disorders.

**Neonatal PCP Induces Transient Misregulation of the Neuronal Surfaceome.** Neuronal activity is well known to modulate gene expression (62). An NMDA antagonist like PCP could thus induce changes in the expression of genes that are key for circuit development. The formation of neuronal networks relies on the proper expression of secreted and membrane proteins, constituting the neuronal surfaceome, that are cues for many developmental steps from cell migration and differentiation to synapse formation. In the olivocerebellar system, several examples of secreted and transmembrane proteins, such as the complement component 1q-related protein family or immunoglobulin superfamily cell-adhesion molecules, have been demonstrated to partially control synapse specificity and territory through specific expression in each PC afferent (63–65). Because of the long-term effect of neonatal PCP administration on the CF/PC synapse, we first aimed to identify the gene expression profile of IONs using the bacterial artificial chromosome – translating ribosome affinity purification (bacTRAP) strategy (66). We used two mouse lines expressing the EGFP (enhanced green fluorescent protein)-L10a transgene under the control of two different drivers: the S100a10 and Cdk6 bacterial artificial chromosomes (BACs) (Fig. 3*A* and *SI Appendix*, Fig. S4). The S100a10 mouse line, previously described (67), drove EGFP-L10a expression in the entire inferior olive (IO) as well as in other brainstem neurons including in the hypoglossal nucleus and dorsal motor nucleus of the vagus nerve. In contrast, EGFP-L10a expression using the Cdk6 BAC driver was restricted to IONs but only in specific subnuclei, namely the medial accessory olive, the dorsal accessory olive, and the dorsal part of the principal accessory olive (Fig. 3*A*). This expression pattern was consistent with data for the Cdk6 line from the GENSAT database (Gene Expression Nervous System Atlas, www.gensat.org). We performed immunoprecipitation of GFP (green fluorescence protein)-tagged polysomes using both mouse lines independently to identify the genes highly expressed in IONs. In both cases, genes known to be expressed in IONs were identified, such as the transcription factor FoxP2 (68) and the serotonin receptor Htr5b (https://mouse.brain-map.org/experiment/show/71247644 and www.gensat.org/). We defined the ION dataset as the ensemble of genes found using both bacTRAP lines. We then compared the ION dataset with the previously published GC dataset (66) to identify genes that would constitute the specific "surfaceome" for each of these two glutamatergic afferents of PCs. A comparison using a fivefold change as a threshold was performed to identify genes clearly

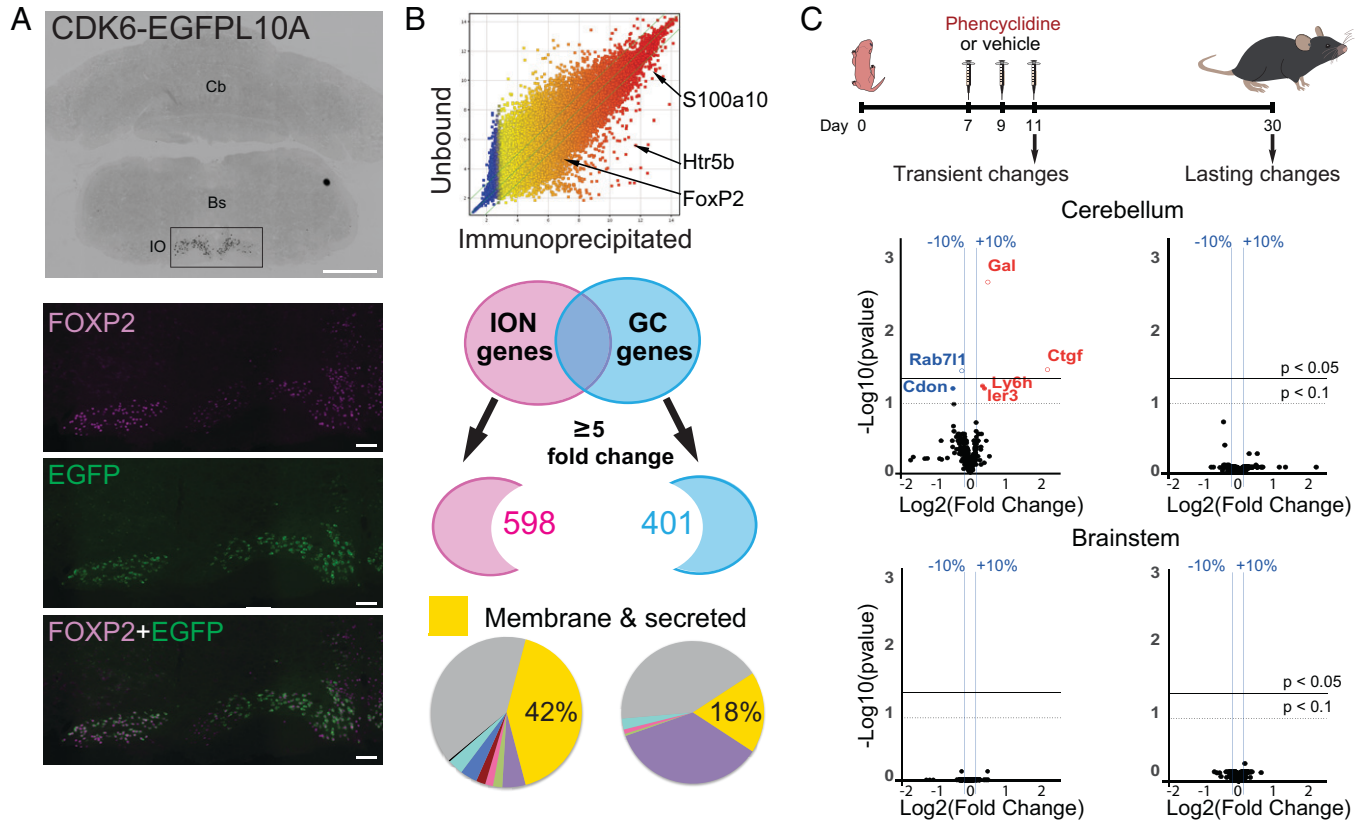


**Fig. 3.** Neonatal PCP administration induces transient translatome changes in the cerebellum. (*A*) Translational profiling of IONS. The Cdk6 BAC driver was used to drive specifically EGFPL10A expression in IONS of the brainstem in adult mice (CDK6-EGFPL10A). Immunostaining with an antibody against Foxp2, an ION-specific transcription factor, confirmed the identity of EGFPL10A-expressing neurons. Bs, brainstem; Cb, cerebellum. (Scale bars: CDK6-EGFPL10A, 1 mm; FOXP2 and EGFP, 100 μm.) (*B*) ION-enriched mRNAs were identified by comparing the immunoprecipitated fraction with the unbound fraction. Known markers of IONs, FoxP2, Htr5b, and S100A10, were identified in the immunoprecipitated fraction. The ION dataset was compared with the GC dataset previously identified (66) to identify input-specific genes (with a threshold of five). DAVID bioinformatics was then used to classify these specific genes according to their cellular localization and to identify the genes coding for the surfaceome (membrane and secreted proteins). (*C*) Experimental design. PCP or vehicle is injected subcutaneously in neonatal mice at P7, P9, and P11. Gene expression changes were analyzed from both cerebellum and brainstem mRNA extracts at either P11, to detect immediate changes after PCP treatment, or at P30, to detect long-lasting changes. Volcano plots are used to represent the changes in gene expression detected in the four groups. Each dot represents the fold change for a gene and the corresponding corrected *P* value [using the Benjamini–Hochberg correction for multiple *t* test comparison (69)]. *y* axis: $-\log_{10}$ of corrected *P* values. *x* axis: $\log_2$ of gene fold change. The top black horizontal lines correspond to an FDR threshold set to 5%, the bottom dotted lines correspond to an FDR set to 10%, and the vertical blue bars correspond to a fold change in gene expression level of 10%. Genes with an FDR < 5% are represented with empty circles.

differentially expressed (differentially expressed genes [DEGs]) (Fig. 3*B*), yielding 598 DEGs for IONs and 401 DEGs for GCs. Classification using the DAVID functional annotation clustering tool identified DEGs coding for membrane and secreted proteins in both datasets, constituting the specific surfaceome for each of the PC excitatory afferents. Of note, the IONs were more complex in the diversity of genes coding for membrane and secreted proteins than GCs (250 genes, 42% vs. 74 genes, 18%, respectively) (Fig. 3*B* and Dataset S1). This might be related to their more complex morphology and the need for molecular cues to control the topographical organization of olivocerebellar connectivity.

Having identified the specific surfaceome of IONs and GCs, we analyzed the expression changes induced by PCP treatment using high-throughput qRT-PCR assessment of these genes in cerebellar and brainstem extracts from P11 animals, right after the last PCP injection, or from P30 animals to detect acute effects and long-lasting changes, respectively (Fig. 3*C* and Dataset S1). After multiple *t* test comparison with a Benjamini–Hochberg false discovery rate (FDR) correction (69), genes that changed significantly by at least 10% were only found in the cerebellum at P11 (Fig. 3*C*), indicating a direct effect of PCP treatment on gene expression patterns in this structure. With an FDR threshold set to 10%, six genes were significantly misregulated: *Ctgf*, *Gal*, *Ier3*, and *Ly6h* were up-regulated, while *Rab7l1* and Cdon were down-regulated (Fig. 3*C* and *SI Appendix*, Fig. S5*A*). Interestingly, all four up-regulated genes were originally enriched in the ION dataset compared with GCs, suggesting that PCP decreases transiently the specification of gene expression in these two PC inputs at a stage when heterosynaptic competition between the two inputs is important for proper development of PC connectivity (70). We then analyzed potential functional links in genes misregulated by PCP in the cerebellum using the string database (https://string-db.org/) that predicts protein–protein interactions, including direct (physical) and indirect (functional) association (71). For this analysis, we included 30 genes with a fold change of at least 10% in the cerebellum that reached significance in multiple *t* tests without correction for FDR, thus accepting a higher rate of false positive (*SI Appendix*, Fig. S5*B*). Predicted interaction was found between seven genes (*Cxcl12*, *Cnr1*, *Gal*, *Oprl1*, *Ctgf*, *Rock2*, and *Igfbp5*) (*SI Appendix*, Fig. S5*B*). Interestingly, *Ctgf* codes for CTGF (also known as CCN2), a secreted protein implicated in extracellular matrix remodeling, cell adhesion, dendritogenesis, and the formation of the neuromuscular junction (72–75). *Ctgf* is expressed in the cerebellum and the brainstem in a pattern that follows synaptic formation and refinement in the olivocerebellar network

(increase in expression from P7 to P21 in the cerebellum and a twofold increase from birth to P14 in the brainstem [*SI Appendix*, Fig. S5*C*]). The increase in *Ctgf* induced by PCP in the cerebellum results in a level of expression equivalent to the one found in the brainstem, potentially impairing the specificity of signaling in the olivocerebellar system. Thus, the misregulation of the surfaceome by PCP in the cerebellum could interfere with normal synapse formation and maturation.

**Overexpression of CTGF during the Second Postnatal Week Is Insufficient to Induce Long-Term Changes in CF/PC Connectivity.** PCP administration leads to acute behavioral effects that peak during the first 2 h, following its pharmacokinetics (76, 77). In the neonatal subchronic PCP model, we also observed acute behavioral effects during the first 2 h following administration of PCP, with pups displaying increased locomotion and motor effects (*SI Appendix*, Fig. S6*A*). These effects disappeared 4 h postinjection (*SI Appendix*, Fig. S6*A*). PCP administration has been reported to change circuit function in several brain areas and is accompanied by the increased activity of various neuronal populations, in particular in the prefrontal cortex and thalamus, shown both by electrophysiological recordings and by increased *cFos* expression, a marker of increased neuronal activity (76, 78, 79). In the olivocerebellar network, acute administration of PCP in the adult rat leads to increased *cFos* expression in the IO, in cerebellar GCs, and in PCs (80). Our analysis using droplet digital PCR showed that *cFos* mRNA expression increases both in the cerebellum and brainstem at P11 after the last PCP injection in the subchronic neonatal PCP model (*SI Appendix*, Fig. S6*B*). This increase disappeared 4 h postinjection, in correlation with the disappearance of acute behavioral effects and the previously published pharmacokinetics of PCP (77). These results suggest that PCP administration in pups transiently increases neuronal activity in the olivocerebellar system and that increased activity in the cerebellum could at least in part lead to the large misregulation of gene expression observed at P11 in PCP pups. To test this, we generated a mouse model enabling chemogenetic control of activity in cerebellar GCs by crossing the floxed hM3Dq (human Gq-coupled M3 muscarinic receptor) knock-in mouse model (81) with the NeuroD1Cre (ND1Cre) mouse line expressing the Cre recombinase in cerebellar GCs (Fig. 4*A*). To mimic the *cFos* increase induced in the PCP model, clozapine *N*-oxide (CNO; 3 mg/kg), the synthetic ligand of hM3Dq, was injected at P7, P9, and P11. This protocol induced, as expected, a strong increase in *cFos* mRNA expression in the cerebellum of P11 double-transgenic animals (Fig. 4*B*). This increase was specific and the result of the combination of both the expression of hM3Dq and CNO administration, as it was absent in control mice not expressing the Cre recombinase or treated with vehicle instead of CNO (Fig. 4*B*). Of the three genes with the biggest misregulation in the PCP subchronic neonatal model (Fig. 3*C*), only the increase of *Ctgf* expression was recapitulated by increasing neuronal activity in the cerebellum using chemogenetics (mean expression relative to *Rpl13a* ± SEM; ND1Cre/WT (ND1Cre/wild-type) controls + CNO: 0.0092 ± 0.0004, $n = 6$; ND1Cre/hM3Dq double heterozygotes + CNO: 0.0283 ± 0.0021, $n = 4$; $P = 0.0095$; Mann–Whitney test) (Fig. 4*B*). Given the reported role of *Ctgf* in the development of the neuromuscular junction (74), we wondered whether its activity-dependent increase is sufficient to induce long-term synaptic defects in cerebellar PCs similar to those induced in the neonatal subchronic PCP model. We thus analyzed the morphology of CF/PC synapses using VGLUT2 immunolabeling, high-resolution confocal imaging, and 3D quantitative analysis in the cerebellum of juvenile ND1Cre/hM3Dq. None of the parameters analyzed, density or volume of VGLUT2 clusters, were changed in the cerebellum of P30 CNO-treated animals compared with controls, regardless of the lobule analyzed (Fig. 4*C*). Thus, activity-dependent *Ctgf* overexpression in the cerebellum during the second postnatal week is not sufficient to recapitulate the long-term changes in CF/PC synapses induced by neonatal PCP administration. Single-molecule fluorescence in situ hybridization experiments on sections from PCP-treated mice at P11 showed that *Ctgf* expression tended to increase in the internal and external granular layers of the cerebellum but that the biggest increase in expression was detected at the surface where meninges are located (*SI Appendix*, Fig. S7). Altogether, our results suggest that while PCP induces an increase in *Ctgf* expression both in the cerebellum and in the meninges, in agreement with its identification as a biomarker in some studies of schizophrenic patients (82, 83), *Ctgf* overexpression in the cerebellum cannot by itself recapitulate the long-term synaptic defects found in PCs in the PCP model, further highlighting the complexity of PCP actions.

## Discussion

The last trimester of pregnancy and the first 2 postnatal years of human development constitute a period of intense synapse formation and network remodeling whose perturbations have been associated with diseases like schizophrenia. In the cerebellum, this period corresponds to the growth and maturation of the PC dendritic tree and its connectivity and is equivalent to the second and third postnatal weeks of rodent development (84). Our study shows that neonatal administration of PCP during this sensitive period correlates with transient molecular changes in genes coding for the neuronal surfaceome in the cerebellum and leads to lasting deficits at the CF/PC synapse in juvenile mice.

**Activity-Dependent and -Independent Consequences of Neonatal PCP Administration.** Cell adhesion molecules that are important for the development of synapses are regulated by neuronal activity (62, 85), and the development of neuronal circuits, including in the cerebellum, implicates activity-dependent mechanisms (86). PCP is a noncompetitive NMDA antagonist and has been shown to affect neuronal activity in various brain regions (76, 78). Both previous data obtained in adult rodents (80) and our results on the neonatal subchronic PCP model show that PCP administration increases neuronal activity in the olivocerebellar network, as assessed by *cFos* mRNA expression. A direct consequence is the transient misregulation of a subset of genes coding for membrane or secreted proteins in the cerebellum. This misregulation occurs during the second postnatal week at a critical period for the development of the synaptic connectivity on cerebellar PCs (86). Our gene expression and pathway analysis pointed to the misregulation of two genes, *Gal* and *Ctgf*, with the most strongly misregulated gene coding for CTGF, an extracellular secreted matrix protein known for its implication in tissue repair, extracellular matrix remodeling, cell survival, cell adhesion, dendritogenesis, and the formation of the neuromuscular junction. CTGF is known to interact with several proteins that are associated with synapse elimination, such as IGF1 (87–89), BMP4 (88, 90, 91), or TGF-$\beta$1 (92). Its pattern of expression during postnatal development also suggested *Ctgf* as a candidate for the regulation of circuit formation. Using chemogenetics, we showed that *Ctgf* increase in the cerebellum, induced by increased neuronal activity, is

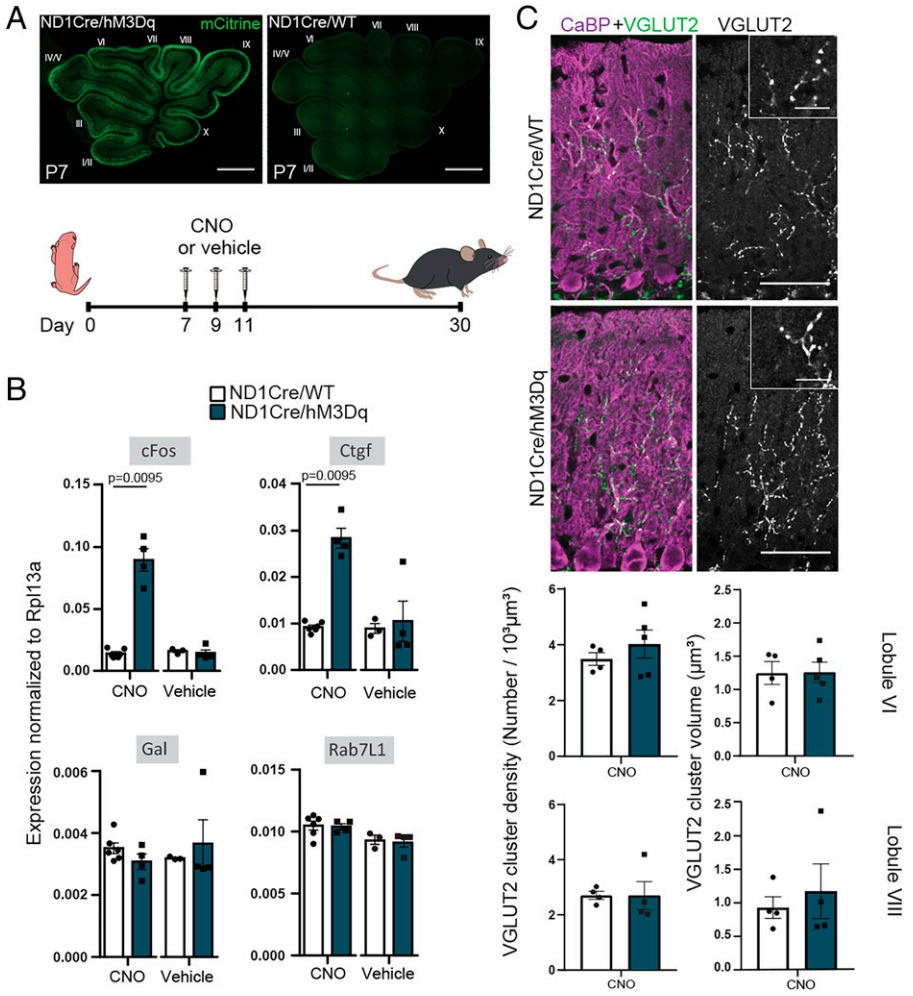


**Fig. 4.** Increased neuronal activity in the cerebellum during postnatal development reproduces the transient increase in *Ctgf* expression but not the long-lasting synaptic effects. (*A*) A chemogenetic strategy was used to test whether an increase in neuronal activity in the cerebellum during the second postnatal week would reproduce the gene expression and synaptic changes seen in the neonatal subchronic PCP model. For this, knock-in mice allowing Cre-dependent expression of the excitatory hM3Dq, along with mCitrine, were crossed with the NeuroD1CRE line that drives Cre recombinase expression in the cerebellar GC lineage (ND1Cre/hM3Dq). CNO or vehicle was injected intraperitoneally at P7, P9, and P11 to reproduce the time course of neonatal PCP injections. Control littermates lacking hM3Dq expression in cerebellar GCs were also analyzed (ND1Cre/WT). Expression of the hM3Dq was monitored using anti-GFP immunostaining to detect mCitrine in slices from the cerebellum of ND1Cre/hM3Dq mice at P7. (*B*) Digital droplet PCR quantifications were used to monitor the gene expression changes induced by increased activity in cerebellar extracts from P11 animals. Subchronic CNO administration leads to a significant increase in *cFos* and *Ctgf* expression in extracts from ND1Cre/hM3Dq mice but not in ND1Cre/WT littermates. *Gal* and *Rab7L1* expression levels remain unchanged. Vehicle treatment does not modify gene expression in either genotype. Gene expression is normalized to *Rpl13a*. Data are presented as mean ± SEM. ND1Cre/WT + CNO: $n = 6$; ND1Cre/HM3Dq + CNO: $n = 4$; ND1Cre/WT + vehicle: $n = 3$; ND1Cre/HM3Dq + vehicle: $n = 4$. Mann–Whitney *U* test. (*C*, *Upper*) CF presynaptic boutons were immunostained with an anti-VGLUT2 antibody (green) and PCs and their dendritic tree were immunostained with an anti-calbindin antibody (magenta) in parasagittal cerebellar sections from ND1Cre/hM3Dq and ND1Cre/WT control mice. *Insets* represent high magnification of VGLUT2 staining. All mice were injected with CNO at P7, P9, and P11. (Scale bars: 50 µm; *Insets*, 12.5 µm.) (*C*, *Lower*) Quantification of the mean density and the mean volume of VGLUT2 puncta revealed no difference in lobules VI and VIII of ND1Cre/hM3Dq mice compared with control mice (mean ± SEM; ND1Cre/WT: $n = 4$ animals; ND1Cre/hM3Dq: $n = 4$ to 5 animals; unpaired Student's *t* test).

not enough to lead to long-term CF/PC synaptic changes. CTGF has been suggested as a plasmatic biomarker in schizophrenia (82, 83); our study indicates that it should be considered more as a biomarker of changes in neuronal activity rather than as a marker of the synaptopathy per se. Misregulation of other surfaceome genes such as *Gal*, the gene coding for the neuropeptide Galanin, is not recapitulated by increased neuronal activity in the cerebellum using chemogenetics and could be involved in the long-lasting PCP-induced changes in CF connectivity. These additional gene expression misregulations could thus be the result of other circuit effects of PCP, in neuronal or cell types other than GCs, or the result of direct gene modulation via mechanisms independent of the PCP blockade of glutamatergic neurotransmission. Finally, the possibility remains that PCP-induced changes in CF connectivity are independent of gene expression modulation in the cerebellum but rather, due to changes in IONs themselves, either directly through modulation of their activity, which might also be increased, as suggested by increased *cFos* expression in the brainstem (*SI Appendix*, Fig. S6*B*) or through PCP-induced changes in molecular signaling in these neurons.

**Deficits in CF/PC Synapses as a Hallmark of Neurodevelopmental Disorders.** The cerebellar cortex, in particular via the integration of multimodal information by PCs, controls the fineness of various cognitive and motor tasks. The synapse between IONs and cerebellar PCs is key for cerebellar computation, as it provides error feedback to the cerebellar cortex and controls the direction of plasticity at PF/PC synapses (93). As such, any defect in this synapse would have profound implications for circuit function and adaptation. In the neonatal subchronic PCP model, the mean volume of CF/PC presynaptic boutons labeled

using the VGLUT2 marker is reduced compared with control conditions, with no change in paired-pulse depression indicating no modifications of the short-term plasticity properties. Similar deficits have been described in models of early postnatal alcohol exposure (94) or genetic models of neurodevelopmental disorders (58, 65, 95). In particular, knockdown of *Bai3*, a gene associated with psychiatric symptoms including in schizophrenia (96–98), induces a reduction in the volume of VGLUT2 boutons (65). CF synaptic defects could thus be a feature of several pathological conditions. In the PCP model, this volume reduction is not accompanied by a reduction in synapse density. On the contrary, an increase in the density of CF/PC boutons is found in juvenile mice treated neonatally with PCP, with a bigger effect in lobule VI than in lobule VIII. This lasting morphological change correlates with an increase in the charge transfer at the CF/PC synapses in a subpopulation of PCs, suggesting that the connectivity between a group of CFs and their target PCs has been strengthened abnormally by the neonatal administration of PCP. One possible explanation would come from the fact that the cerebellum has an asynchronous development; for example, dendritogenesis in lobules I and X occurs earlier than in lobules VI, VII, and VIII (99). In the neonatal PCP model, PCP is injected at P7, P9, and P11 and might perturb specific regions of the cerebellum because of their asynchronous maturation. Given that the olivocerebellar network is organized topographically, this lobule-specific effect could have consequences on cerebellar computation in specific behavioral tasks. This is particularly relevant for neurodevelopmental disorders like schizophrenia that are not associated with a broad and homogeneous effect on behavior and cognition. Furthermore, this type of selective deficits could render the system much more susceptible to secondary insults during circuit maturation, leading to specific behavioral symptoms, in line with the multifactorial etiology of disorders such as schizophrenia. Synaptic deficits in postmortem tissues and genetic association with mutations in synaptic genes indicate that schizophrenia is a synaptopathy. While it is considered that schizophrenia has a developmental origin (100), little is known about the precise developmental mechanisms leading to synaptic deficits in this disease. While initially thought to be essentially a motor task–related structure, many studies highlight the role of the cerebellum in cognition (35, 36, 101–104). The cerebellum emerges now as a potential actor of psychiatric disorders, such as autism spectrum disorders (105, 106) or schizophrenia (107). Together with our demonstration of CF deficits in the neonatal PCP model, this warrants the search for cerebellar synaptic deficits in postmortem tissue from schizophrenic patients and further studies of cerebellar involvement in the pathophysiology of this disease.

## Materials and Methods

**Animals.** All animal protocols were approved by the Comité Régional d'Ethique en Expérimentation Animale (no. 21815), and animals were housed in authorized facilities of the Center for Interdisciplinary Research in Biology (C75 05 12). PCP (Phencyclidine hydrochloride; no. P3029; Merck KGaA; 10 mg/kg diluted in saline solution) or vehicle (saline solution) was injected subcutaneously at P7, P9, and P11 in C57BL6/J mice.

**Translational Profiling of IONS** The RP23-454P8 BAC driver was modified according to previously published protocols (108) to drive the expression of the *EGFPL10a* transgene under the regulatory elements of the *Cdk6* gene. The mouse line Cdk6-EGFPL10A was then generated by random transgenesis via injection of the modified BAC in FVB/N mouse oocytes (mouse oocyte injection performed at the Service des Animaux Transgéniques-UPS44, National Center for Scientific Research [France]).

The gene expression profile of IONS was identified using bacTRAP purification of EGFP-tagged polysomes from the Cdk6-EGFPL10A and S100A10-EGFPL10A mouse lines according to previously published protocols (66). For each set, brainstems were dissected from 20 adult mice (both males and females). Four independent sets of immunopurification were performed for the Cdk6-EGFPL10A line, and three sets of immunopurification were performed for the S100A10-EGFPL10A line. RNA quantity and quality were determined with a Nanodrop spectrophotometer and Agilent 2100 Bioanalyzer. For each sample, total RNA was amplified with the Affymetrix two-cycle amplification kit and hybridized to Affymetrix 430 2.0 microarrays according to the manufacturer's instructions (for the Cdk6-EGFPL10A line at the Plateforme Biopuces et Séquençage, Institut de Génétique et de Biologie Moléculaire et Cellulaire; for the S100A10-EGFPL10A line at the Rockefeller University facility). Analysis was performed using the GeneSpringGX software (version 11.5). First, mRNAs expressed and enriched in IONs compared with the rest of the brainstem were identified by comparing immunoprecipitated mRNAs with the unbound fraction as described in refs. 66 and 109 using a threshold of 1.5 to obtain a baseline level of expression. Second, the immunoprecipitated fraction from IONs was compared with the immunoprecipitated fraction from the NeuroD1-EGFPL10A line (66) corresponding to the GCs using a high threshold (greater than or equal to five) to obtain a high level of input cell specificity. Both lists were then compared to identify common genes that constituted the final gene list for each cell type.

**Statistical Analysis.** Data were analyzed using GraphPad Prism for statistics. Values are given as mean ± SEM.

Normality was estimated using the d'Agostino Pearson or Shapiro–Wilk normality test. The means between two conditions were compared using the unpaired Student's *t* test when both datasets followed a normal law and when the variances were not significantly different (*F* test to compare variance). When data were normally distributed but their variances were different, Welch's *t* test was used. When the dataset did not follow a normal law, the means were compared using a Mann–Whitney nonparametric test. In order to identify and remove potential outliers in our data, we used the robust regression and outlier removal test, with a Q fixed at 1%. One outlier was identified in the VGLUT2 volume quantification (indicated in the data file).

Detailed experimental methods are in *SI Appendix*.

**Data Availability.** All study data are included in the article and/or supporting information.

**ACKNOWLEDGMENTS.** We thank P. Marin and B. Ducos for helpful discussions, E. Schmidt for the S100a10 mouse line, and Mary Beth Hatten for the NeuroD1Cre line. We also thank Pierre Yger for help with the SpyKING CIRCUS software, Philippe Mailly for the quantification plug-in used for the RNAscope experiment, France Maloumian for some infographics, and the personnel from the Center for Interdisciplinary Research in Biology animal and imaging facilities. High-throughput qPCR was carried out on the qPCR-Haut Débit-Genomic Paris Centre platform supported by grants from Région Ile-de-France. This work was supported by funding from Ecole Normale Supérieure Labex MemoLife Grant ANR-10-LABX-54 MEMO LIFE (to A.U. and K.I.), Association Française du Syndrome de Rett (to F.S.), Boehringer Ingelheim Federation of European Neuroscience Societies Award 2010 (to F.S.), ATIP-AVENIR Program RSE11005JSA (to F.S.), Idex Grant PSL ANR-10-IDEX-0001-02 PSL* (to F.S.), Fondation pour la Recherche Médicale Equipe Grant FRM DEQ20150331748 (to F.S.), and European Research Council Consolidator Grant SynID 724601 (to F.S.). K.I. was supported by a PhD grant from the Ecole des Neurosciences de Paris. Part of this manuscript appeared as part of the dissertation of M.V.

Author affiliations: [a]Center for Interdisciplinary Research in Biology (CIRB), College de France, CNRS, INSERM, Université PSL, 75005 Paris, France; [b]Plateforme qPCR-Haut Débit-Genomic Paris Centre, Institut de Biologie de l'Ecole Normale Supérieure, 75005 Paris, France; [c]Laboratory of Molecular Biology, The Rockefeller University, New York, NY 10065; [d]HHMI, The Rockefeller University, New York, NY 10065; and [e]Institute for Functional Genomics, University of Montpellier, CNRS, INSERM, 34094 Montpellier, France

Author contributions: N.H. and F.S. designed research; M.V., B.U.-C., S.M.S., M.A.P., A.U., K.I., M.D., J.P.D., and F.S. performed research; N.H. and C.B. contributed new reagents/analytic tools; M.V., B.U.-C., S.M.S., M.A.P., A.U., K.I., and F.S. analyzed data; M.V., B.U.-C., S.M.S., M.A.P., A.U., K.I., J.P.D., N.H., C.B., and F.S. read the manuscript; and M.V. and F.S. wrote the paper.

1. E. F. Domino, E. D. Luby, Phencyclidine/schizophrenia: One view toward the past, the other to the future. *Schizophr. Bull.* **38**, 914–919 (2012).
2. D. Lodge, M. S. Mercier, Ketamine and phencyclidine: The good, the bad and the unexpected. *Br. J. Pharmacol.* **172**, 4254–4276 (2015).
3. C. A. Jones, D. J. Watson, K. C. Fone, Animal models of schizophrenia. *Br. J. Pharmacol.* **164**, 1162–1194 (2011).
4. C. Wang *et al.*, Long-term behavioral and neurodegenerative effects of perinatal phencyclidine administration: Implications for schizophrenia. *Neuroscience* **107**, 535–550 (2001).
5. A. Nakatani-Pawlak, K. Yamaguchi, Y. Tatsumi, H. Mizoguchi, Y. Yoneda, Neonatal phencyclidine treatment in mice induces behavioral, histological and neurochemical abnormalities in adulthood. *Biol. Pharm. Bull.* **32**, 1576–1583 (2009).
6. J.-P. Terranova *et al.*, SSR181507, a dopamine D(2) receptor antagonist and 5-HT(1A) receptor agonist, alleviates disturbances of novelty discrimination in a social context in rats, a putative model of selective attention deficit. *Psychopharmacology (Berl.)* **181**, 134–144 (2005).
7. J. Meffre *et al.*, 5-HT(6) receptor recruitment of mTOR as a mechanism for perturbed cognition in schizophrenia. *EMBO Mol. Med.* **4**, 1043–1056 (2012).
8. N. E. Clifton, N. Morisot, S. Girardon, M. J. Millan, F. Loiseau, Enhancement of social novelty discrimination by positive allosteric modulators at metabotropic glutamate 5 receptors: Adolescent administration prevents adult-onset deficits induced by neonatal treatment with phencyclidine. *Psychopharmacology (Berl.)* **225**, 579–594 (2013).
9. N. C. Anastasio, K. M. Johnson, Atypical anti-schizophrenic drugs prevent changes in cortical N-methyl-D-aspartate receptors and behavior following sub-chronic phencyclidine administration in developing rat pups. *Pharmacol. Biochem. Behav.* **90**, 569–577 (2008).
10. C. Kjaerby, C. Bundgaard, K. Fejgin, U. Kristiansen, N. O. Dalby, Repeated potentiation of the metabotropic glutamate receptor 5 and the alpha 7 nicotinic acetylcholine receptor modulates behavioural and GABAergic deficits induced by early postnatal phencyclidine (PCP) treatment. *Neuropharmacology* **72**, 157–168 (2013).
11. F. Rahbar, A. Fomufod, D. White, L. S. Westney, Impact of intrauterine exposure to phencyclidine (PCP) and cocaine on neonates. *J. Natl. Med. Assoc.* **85**, 349–352 (1993).
12. S. I. Deutsch, J. Mastropaolo, R. B. Rosse, Neurodevelopmental consequences of early exposure to phencyclidine and related drugs. *Clin. Neuropharmacol.* **21**, 320–332 (1998).
13. J. L. Rapoport, J. N. Giedd, N. Gogtay, Neurodevelopmental model of schizophrenia: Update 2012. *Mol. Psychiatry* **17**, 1228–1238 (2012).
14. L. A. Glantz, D. A. Lewis, Reduction of synaptophysin immunoreactivity in the prefrontal cortex of subjects with schizophrenia. Regional and diagnostic specificity. *Arch. Gen. Psychiatry* **54**, 660–669 (1997).
15. C. N. Karson *et al.*, Alterations in synaptic proteins and their encoding mRNAs in prefrontal cortex in schizophrenia: A possible neurochemical basis for 'hypofrontality.' *Mol. Psychiatry* **4**, 39–45 (1999).
16. S. L. Eastwood, P. J. Harrison, Decreased expression of vesicular glutamate transporter 1 and complexin II mRNAs in schizophrenia: Further evidence for a synaptic pathology affecting glutamate neurons. *Schizophr. Res.* **73**, 159–172 (2005).
17. E. Scarr, L. Gray, D. Keriakous, P. J. Robinson, B. Dean, Increased levels of SNAP-25 and synaptophysin in the dorsolateral prefrontal cortex in bipolar I disorder. *Bipolar Disord.* **8**, 133–143 (2006).
18. S. M. Purcell *et al.*, A polygenic burden of rare disruptive mutations in schizophrenia. *Nature* **506**, 185–190 (2014).
19. S. Ripke *et al.*; Schizophrenia Working Group of the Psychiatric Genomics Consortium, Biological insights from 108 schizophrenia-associated genetic loci. *Nature* **511**, 421–427 (2014).
20. E. F. Osimo, K. Beck, T. Reis Marques, O. D. Howes, Synaptic loss in schizophrenia: A meta-analysis and systematic review of synaptic protein and mRNA measures. *Mol. Psychiatry* **24**, 549–561 (2019).
21. R. C. Roberts, L. A. Gaither, F. J. Peretti, B. Lapidus, D. J. Chute, Synaptic organization of the human striatum: A postmortem ultrastructural study. *J. Comp. Neurol.* **374**, 523–534 (1996).
22. L. A. Glantz, D. A. Lewis, Decreased dendritic spine density on prefrontal cortical pyramidal neurons in schizophrenia. *Arch. Gen. Psychiatry* **57**, 65–73 (2000).
23. G. Rosoklija *et al.*, Structural abnormalities of subicular dendrites in subjects with schizophrenia and mood disorders: Preliminary findings. *Arch. Gen. Psychiatry* **57**, 349–356 (2000).
24. G. P. Reynolds, Z. Abdul-Monim, J. C. Neill, Z.-J. Zhang, Calcium binding protein markers of GABA deficits in schizophrenia–Postmortem studies and animal models. *Neurotox. Res.* **6**, 57–61 (2004).
25. T. A. Jenkins, M. K. Harte, C. E. McKibben, J. J. Elliott, G. P. Reynolds, Disturbances in social interaction occur along with pathophysiological deficits following sub-chronic phencyclidine administration in the rat. *Behav. Brain Res.* **194**, 230–235 (2008).
26. A. Mouri, Y. Noda, T. Enomoto, T. Nabeshima, Phencyclidine animal models of schizophrenia: Approaches from abnormality of glutamatergic neurotransmission and neurodevelopment. *Neurochem. Int.* **51**, 173–184 (2007).
27. S. S. Kaalund *et al.*, Differential expression of parvalbumin in neonatal phencyclidine-treated rats and socially isolated rats. *J. Neurochem.* **124**, 548–557 (2013).
28. B. Yu, C. Wang, J. Liu, K. M. Johnson, J. P. Gallagher, Adaptation to chronic PCP results in hyperfunctional NMDA and hypofunctional GABA(A) synaptic receptors. *Neuroscience* **113**, 1–10 (2002).
29. T. Nomura *et al.*, Subchronic phencyclidine treatment in adult mice increases GABAergic transmission and LTP threshold in the hippocampus. *Neuropharmacology* **100**, 90–97 (2016).
30. C. Kjaerby, B. V. Broberg, U. Kristiansen, N. O. Dalby, Impaired GABAergic inhibition in the prefrontal cortex of early postnatal phencyclidine (PCP)-treated rats. *Cereb. Cortex* **24**, 2522–2532 (2014).
31. J. D. Schmahmann, An emerging concept. The cerebellar contribution to higher function. *Arch. Neurol.* **48**, 1178–1187 (1991).
32. C. J. Stoodley, J. D. Schmahmann, Evidence for topographic organization in the cerebellum of motor control versus cognitive and affective processing. *Cortex* **46**, 831–844 (2010).
33. C. Rochefort *et al.*, Cerebellum shapes hippocampal spatial code. *Science* **334**, 385–389 (2011).
34. X. Guell, F. Hoche, J. D. Schmahmann, Metalinguistic deficits in patients with cerebellar dysfunction: Empirical support for the dysmetria of thought theory. *Cerebellum* **14**, 50–58 (2015).
35. M. J. Wagner, T. H. Kim, J. Savall, M. J. Schnitzer, L. Luo, Cerebellar granule cells encode the expectation of reward. *Nature* **544**, 96–100 (2017).
36. A. Badura *et al.*, Normal cognitive and social development require posterior cerebellar activity. *eLife* **7**, e36401 (2018).
37. D. R. Weinberger, J. E. Kleinman, D. J. Luchins, L. B. Bigelow, R. J. Wyatt, Cerebellar pathology in schizophrenia: A controlled postmortem study. *Am. J. Psychiatry* **137**, 359–361 (1980).
38. N. C. Andreasen *et al.*, Schizophrenia and cognitive dysmetria: A positron-emission tomography study of dysfunctional prefrontal-thalamic-cerebellar circuitry. *Proc. Natl. Acad. Sci. U.S.A.* **93**, 9985–9990 (1996).
39. T. Moberget *et al.*, Cerebellar gray matter volume is associated with cognitive function and psychopathology in adolescence. *Biol. Psychiatry* **86**, 65–75 (2019).
40. D. Hirjak, P. A. Thomann, K. M. Kubera, B. Stieltjes, R. C. Wolf, Cerebellar contributions to neurological soft signs in healthy young adults. *Eur. Arch. Psychiatry Clin. Neurosci.* **266**, 35–41 (2016).
41. T. H. Wassink, N. C. Andreasen, P. Nopoulos, M. Flaum, Cerebellar morphology as a predictor of symptom and psychosocial outcome in schizophrenia. *Biol. Psychiatry* **45**, 41–48 (1999).
42. R. Prikryl, E. Ceskova, T. Kasparek, H. Kucerova, Neurological soft signs and their relationship to 1-year outcome in first-episode schizophrenia. *Eur. Psychiatry* **22**, 499–504 (2007).
43. H. Picard, I. Amado, S. Mouchet-Mages, J. P. Olié, M. O. Krebs, The role of the cerebellum in schizophrenia: An update of clinical, cognitive, and functional evidences. *Schizophr. Bull.* **34**, 155–172 (2008).
44. R. O. Brady Jr. *et al.*, Cerebellar-prefrontal network connectivity and negative symptoms in schizophrenia. *Am. J. Psychiatry* **176**, 512–520 (2019).
45. C. Bidoret, G. Bouvier, A. Ayon, G. Szapiro, M. Casado, Properties and molecular identity of NMDA receptors at synaptic and non-synaptic inputs in cerebellar molecular layer interneurons. *Front. Synaptic Neurosci.* **7**, 1 (2015).
46. R. D. Burgoyne, M. E. Graham, M. Cambray-Deakin, Neurotrophic effects of NMDA receptor activation on developing cerebellar granule cells. *J. Neurocytol.* **22**, 689–695 (1993).
47. M. Farrant, D. Feldmeyer, T. Takahashi, S. G. Cull-Candy, NMDA-receptor channel diversity in the developing cerebellum. *Nature* **368**, 335–339 (1994).
48. X.-W. Chen *et al.*, DTNBP1, a schizophrenia susceptibility gene, affects kinetics of transmitter release. *J. Cell Biol.* **181**, 791–801 (2008).
49. C. Piochon *et al.*, NMDA receptor contribution to the climbing fiber response in the adult mouse Purkinje cell. *J. Neurosci.* **27**, 10797–10809 (2007).
50. A. Contestabile, Cerebellar granule cells as a model to study mechanisms of neuronal apoptosis or survival in vivo and in vitro. *Cerebellum* **1**, 41–55 (2002).
51. S. Rabacchi, Y. Bailly, N. Delhaye-Bouchaud, J. Mariani, Involvement of the N-methyl D-aspartate (NMDA) receptor in synapse elimination during cerebellar development. *Science* **256**, 1823–1825 (1992).
52. G. Bouvier *et al.*, Burst-dependent bidirectional plasticity in the cerebellum is driven by presynaptic NMDA receptors. *Cell Rep.* **15**, 104–116 (2016).
53. J. Mapelli, D. Gandolfi, A. Vilella, M. Zoli, A. Bigiani, Heterosynaptic GABAergic plasticity bidirectionally driven by the activity of pre- and postsynaptic NMDA receptors. *Proc. Natl. Acad. Sci. U.S.A.* **113**, 9898–9903 (2016).
54. T. Moberget, R. B. Ivry, Prediction, psychosis, and the cerebellum. *Biol. Psychiatry Cogn. Neurosci. Neuroimaging* **4**, 820–831 (2019).
55. M. E. van der Heijden *et al.*, Maturation of Purkinje cell firing properties relies on neurogenesis of excitatory neurons. *eLife* **10**, 1–37 (2021).
56. G. R. Holt, W. R. Softky, C. Koch, R. J. Douglas, Comparison of discharge variability in vitro and in vivo in cat visual cortex neurons. *J. Neurophysiol.* **75**, 1806–1814 (1996).
57. C. J. Stoodley, The cerebellum and cognition: Evidence from functional imaging studies. *Cerebellum* **11**, 352–365 (2012).
58. B. Zhang *et al.*, Neuroligins sculpt cerebellar purkinje-cell circuits by differential control of distinct classes of synapses. *Neuron* **87**, 781–796 (2015).
59. G. Gonzalez-Burgos, T. Hashimoto, D. A. Lewis, Alterations of cortical GABA neurons and network oscillations in schizophrenia. *Curr. Psychiatry Rep.* **12**, 335–344 (2010).
60. N. Radhu *et al.*, Evidence for inhibitory deficits in the prefrontal cortex in schizophrenia. *Brain* **138**, 483–497 (2015).
61. A. Konnerth, I. Llano, C. M. Armstrong, Synaptic currents in cerebellar Purkinje cells. *Proc. Natl. Acad. Sci. U.S.A.* **87**, 2662–2665 (1990).
62. D. H. Ebert, M. E. Greenberg, Activity-dependent neuronal signalling and autism spectrum disorder. *Nature* **493**, 327–337 (2013).
63. H. Hirai *et al.*, Cbln1 is essential for synaptic integrity and plasticity in the cerebellum. *Nat. Neurosci.* **8**, 1534–1541 (2005).
64. W. Kakegawa *et al.*, Anterograde C1ql1 signaling is required in order to determine and maintain a single-winner climbing fiber in the mouse cerebellum. *Neuron* **85**, 316–329 (2015).
65. S. M. Sigoillot *et al.*, The secreted protein C1QL1 and its receptor BAI3 control the synaptic connectivity of excitatory inputs converging on cerebellar Purkinje cells. *Cell Rep.* **10**, 820–832 (2015).
66. J. P. Doyle *et al.*, Application of a translational profiling approach for the comparative analysis of CNS cell types. *Cell* **135**, 749–762 (2008).
67. E. F. Schmidt *et al.*, Identification of the cortical neurons that mediate antidepressant responses. *Cell* **149**, 1152–1163 (2012).
68. C. S. L. Lai, D. Gerrelli, A. P. Monaco, S. E. Fisher, A. J. Copp, FOXP2 expression during brain development coincides with adult sites of pathology in a severe speech and language disorder. *Brain* **126**, 2455–2462 (2003).
69. Y. Benjamini, Y. Hochberg, Controlling the false discovery rate: A practical and powerful approach to multiple testing. *J. R. Stat. Soc. B* **57**, 289–300 (1995).
70. R. Ichikawa *et al.*, Territories of heterologous inputs onto Purkinje cell dendrites are segregated by mGluR1-dependent parallel fiber synapse elimination. *Proc. Natl. Acad. Sci. U.S.A.* **113**, 2282–2287 (2016).
71. D. Szklarczyk *et al.*, The STRING database in 2017: Quality-controlled protein-protein association networks, made broadly accessible. *Nucleic Acids Res.* **45**, D362–D368 (2017).
72. M. Hoshijima *et al.*, CT domain of CCN2/CTGF directly interacts with fibronectin and enhances cell adhesion of chondrocytes through integrin $\alpha 5\beta 1$. *FEBS Lett.* **580**, 1376–1382 (2006).
73. K. Khodosevich *et al.*, Connective tissue growth factor regulates interneuron survival and information processing in the olfactory bulb. *Neuron* **79**, 1136–1151 (2013).
74. B. Ohkawara *et al.*, CTGF/CCN2 facilitates LRP4-mediated formation of the embryonic neuromuscular junction. *EMBO Rep.* **21**, e48462 (2020).

75. Y. Ramazani *et al.*, Connective tissue growth factor (CTGF) from basics to clinics. *Matrix Biol.* **68–69**, 44–66 (2018).
76. M. Amat-Foraster *et al.*, Modulation of thalamo-cortical activity by the NMDA receptor antagonists ketamine and phencyclidine in the awake freely-moving rat. *Neuropharmacology* **158**, 107745 (2019).
77. F. Gastambide, S. N. Mitchell, T. W. Robbins, M. D. Tricklebank, G. Gilmour, Temporally distinct cognitive effects following acute administration of ketamine and phencyclidine in the rat. *Eur. Neuropsychopharmacol.* **23**, 1414–1422 (2013).
78. L. Kargieman, N. Santana, G. Mengod, P. Celada, F. Artigas, Antipsychotic drugs reverse the disruption in prefrontal cortex function produced by NMDA receptor blockade with phencyclidine. *Proc. Natl. Acad. Sci. U.S.A.* **104**, 14843–14848 (2007).
79. A. Castañé, N. Santana, F. Artigas, PCP-based mice models of schizophrenia: Differential behavioral, neurochemical and cellular effects of acute and subchronic treatments. *Psychopharmacology (Berl.)* **232**, 4085–4097 (2015).
80. R. Näkki, J. Koistinaho, F. R. Sharp, S. M. Sagar, Cerebellar toxicity of phencyclidine. *J. Neurosci.* **15**, 2097–2108 (1995).
81. G. M. Alexander *et al.*, Remote control of neuronal activity in transgenic mice expressing evolved G protein-coupled receptors. *Neuron* **63**, 27–39 (2009).
82. E. Schwarz *et al.*, Validation of a blood-based laboratory test to aid in the confirmation of a diagnosis of schizophrenia. *Biomark. Insights* **5**, 39–47 (2010).
83. Y. Li *et al.*, Biomarker identification and effect estimation on schizophrenia - A high dimensional data analysis. *Front. Public Health* **3**, 75 (2015).
84. N. Zecevic, P. Rakic, Differentiation of Purkinje cells and their relationship to other components of developing cerebellar cortex in man. *J. Comp. Neurol.* **167**, 27–47 (1976).
85. R. D. Fields, K. Itoh, Neural cell adhesion molecules in activity-dependent development and synaptic plasticity. *Trends Neurosci.* **19**, 473–480 (1996).
86. K. Hashimoto, M. Kano, Synapse elimination in the developing cerebellum. *Cell. Mol. Life Sci.* **70**, 4667–4680 (2013).
87. H.-S. Kim *et al.*, Identification of a family of low-affinity insulin-like growth factor binding proteins (IGFBPs): Characterization of connective tissue growth factor as a member of the IGFBP superfamily. *Proc. Natl. Acad. Sci. U.S.A.* **94**, 12981–12986 (1997).
88. J. G. Abreu, N. I. Ketpura, B. Reversade, E. M. De Robertis, Connective-tissue growth factor (CTGF) modulates cell signalling by BMP and TGF-$\beta$. *Nat. Cell Biol.* **4**, 599–604 (2002).
89. S. Kakizawa, K. Yamada, M. Iino, M. Watanabe, M. Kano, Effects of insulin-like growth factor I on climbing fibre synapse elimination during cerebellar development. *Eur. J. Neurosci.* **17**, 545–554 (2003).
90. A. Kalinovsky *et al.*, Development of axon-target specificity of ponto-cerebellar afferents. *PLoS Biol.* **9**, e1001013 (2011).
91. T. Higashi, S. Tanaka, T. Iida, S. Okabe, Synapse elimination triggered by BMP4 exocytosis and presynaptic BMP receptor activation. *Cell Rep.* **22**, 919–929 (2018).
92. A. R. Bialas, B. Stevens, TGF-$\beta$ signaling regulates neuronal C1q expression and developmental synaptic refinement. *Nat. Neurosci.* **16**, 1773–1782 (2013).
93. J. L. Raymond, J. F. Medina, Computational principles of supervised learning in the cerebellum. *Annu. Rev. Neurosci.* **41**, 233–253 (2018).
94. D. R. Pierce, A. Hayar, D. K. Williams, K. E. Light, Olivary climbing fiber alterations in PN40 rat cerebellum following postnatal ethanol exposure. *Brain Res.* **1378**, 54–65 (2011).
95. H. L. Cha *et al.*, Deletion of the $\alpha$ subunit of the heterotrimeric Go protein impairs cerebellar cortical development in mice. *Mol. Brain* **12**, 57 (2019).
96. P. DeRosse *et al.*, The genetics of symptom-based phenotypes: Toward a molecular classification of schizophrenia. *Schizophr. Bull.* **34**, 1047–1053 (2008).
97. H.-M. Liao *et al.*, Identification and characterization of three inherited genomic copy number variations associated with familial schizophrenia. *Schizophr. Res.* **139**, 229–236 (2012).
98. E. S. Lips *et al.*; International Schizophrenia Consortium, Functional gene group analysis identifies synaptic gene groups as risk factor for schizophrenia. *Mol. Psychiatry* **17**, 996–1006 (2012).
99. C. Sotelo, Cellular and genetic regulation of the development of the cerebellar system. *Prog. Neurobiol.* **72**, 295–339 (2004).
100. D. R. Weinberger, The neurodevelopmental origins of schizophrenia in the penumbra of genomic medicine. *World Psychiatry* **16**, 225–226 (2017).
101. J. D. Schmahmann, The cerebellum and cognition. *Neurosci. Lett.* **688**, 62–75 (2019).
102. N. Sendhilnathan, M. Semework, M. E. Goldberg, A. E. Ipata, Neural correlates of reinforcement learning in mid-lateral cerebellum. *Neuron* **106**, 188–198.e5 (2020).
103. L. Rondi-Reig, A.-L. Paradis, J. M. Lefort, B. M. Babayan, C. Tobin, How the cerebellum may monitor sensory information for spatial representation. *Front. Syst. Neurosci.* **8**, 205 (2014).
104. I. Carta, C. H. Chen, A. L. Schott, S. Dorizan, K. Khodakhah, Cerebellar modulation of the reward circuitry and social behavior. *Science* **363**, eaav0581 (2019).
105. E. B. E. Becker, C. J. Stoodley, "Autism spectrum disorder and the cerebellum" in *Neurobiology of Autism*, G. Konopka, Ed. (International Review of Neurobiology, Academic Press, 2013), pp. 1–34.
106. S. S.-H. Wang, A. D. Kloth, A. Badura, The cerebellum, sensitive periods, and autism. *Neuron* **83**, 518–532 (2014).
107. N. C. Andreasen, R. Pierson, The role of the cerebellum in schizophrenia. *Biol. Psychiatry* **64**, 81–88 (2008).
108. S. Gong, L. Kus, N. Heintz, Rapid bacterial artificial chromosome modification for large-scale mouse transgenesis. *Nat. Protoc.* **5**, 1678–1696 (2010).
109. J. D. Dougherty, E. F. Schmidt, M. Nakajima, N. Heintz, Analytical approaches to RNA profiling data for the identification of genes enriched in specific cells. *Nucleic Acids Res.* **38**, 4218–4230 (2010).